FILE COPY
No. 1

FILE COPY
To be returned to the Files of
Ames Aeronautical Laboratory
National Advisory Committee
for Aeronautics
Moffett Field, Calif.

TN 741

615.4
Kettett
6-15-11

TECHNICAL NOTES

NATIONAL ADVISORY COMMITTEE FOR AERONAUTICS

No. 741

OBSERVATIONS IN FLIGHT OF THE REGION OF STALLED FLOW OVER THE BLADES OF AN AUTOGIRO ROTOR

By F. J. Bailey, Jr., and F. B. Gustafson
Langley Memorial Aeronautical Laboratory

Washington
December 1939

NATIONAL ADVISORY COMMITTEE FOR AERONAUTICS

TECHNICAL NOTE NO. 741

OBSERVATIONS IN FLIGHT OF THE REGION OF STALLED FLOW OVER THE BLADES OF AN AUTOGIRO ROTOR

By F. J. Bailey, Jr., and F. B. Gustafson

SUMMARY

The flow over the inner halves of the rotor blades on a Kellett YG-1B autogiro was investigated in flight by making camera records of the motion of silk streamers attached to the upper surfaces of the blades. These records were analyzed to determine the boundaries of the region within which the flow over the blade sections was stalled for various tip-speed ratios. For the sake of comparison, corresponding theoretical boundaries were obtained. Both the size of the stalled area and its rate of growth with increasing tip-speed ratio were found to be larger than the theory predicted, although experiment agreed with theory with regard to shape and general location of the stalled area. The stalled region may be an important factor in both the rotor lift-drag ratio and the blade flapping motion at the higher tip-speed ratios. The method of study used in this paper should be useful in further studies of the problem, including the reduction of the size of the region.

INTRODUCTION

The theoretical analysis of the autogiro rotor, developed by Glauert, Lock, and Wheatley, includes expressions from which the angle of attack of a blade element at any position in the rotor disk can be calculated. These expressions indicate the existence of three distinct regions on the rotor disk. In one of these regions, the blade elements are unstalled; in another, they are stalled; and, in the third, they are subjected to a reversed flow, with the air moving from trailing edge to leading edge. The boundaries of the stalled region, which lies between the other two regions on the rotor disk, can be calculated from the theoretical expressions, provided that the angle of attack at stall of the blade airfoil section is known.

The size, the shape, and the importance of the stalled region as obtained from the theory are not quite accurate because: (1) the blade elements passing through the region are subjected to high angles of attack for an extremely short interval; (2) the angle of attack at stall can be markedly affected by the conditions of operation in the rotor, namely, the large and rapid changes in angle of attack, angle of yaw, and velocity; and (3) the local values of the inflow velocity are known to depart considerably from the mean value used in the theory.

Calculations indicate that the profile drag of stalled blade elements may appreciably lower the maximum lift-drag ratio of a rotor, if the boundaries of the stalled region differ materially from those predicted by theory. For this reason, the N.A.C.A. has recently attempted to establish the boundaries of this region by photographic observations of the motion of tufts attached to the upper surfaces of the blades. The investigation was made at Langley Field during December 1938 on a Kellett YG-1B autogiro.

APPARATUS AND METHODS

The YG-1B autogiro is a three-blade direct-control wingless autogiro, identical in general arrangement to the Kellett KD-1 autogiro described in reference 1. The characteristics of the rotor, particularly the blade motion, are somewhat different owing to the addition of upturned trailing-edge tabs over the outer part of the blades.

The motion of the tufts was observed by means of a motion-picture camera mounted on the top of the rotor hub and aimed outward over one of the blades at approximately 30 percent of the blade chord. Frames typical of the ones made in these observations are shown in figure 1. The azimuth position of the camera and the blade at the instant each picture was taken was established by making all flights directly away from the sun at a time of day when the sun was low enough to appear on the film. Constant camera speed and rotor speed were assumed between successive images of the sun. Records from 2 to 9 seconds in length were taken in steady glides at indicated air speeds from 40 to 90 miles per hour, corresponding to tip-speed ratios from 0.16 to 0.32. The flight altitudes ranged from 1,500 to 3,000 feet.

The tufts, which were made up of red silk ribbons 1/4 inch wide and 3-1/2 inches long, were mounted in pairs at various radii on the upper surface of the blade. The forward tuft of each pair was attached a little ahead of the maximum thickness of the blade, that is, at about 25 percent of the chord; the rear tuft was attached at about 70 percent of the chord and reached almost to the trailing edge of the blade. The forward tuft was placed 3 inches inboard of the rear tuft; the average position was used as the radius. In the course of the tests, pairs of tufts were placed at radii of $x = 0.145$, 0.250, 0.375, and 0.500, where x is the ratio of the station radius to the tip radius (20 ft.). In addition, a tuft was attached just ahead of the trailing edge at $x = 0.250$ in one flight and 0.375 in another. In the first flight, a single tuft was placed at a 15-foot radius but could not be clearly detected in the records; hence, the 10-foot radius was the largest to be read. In order to enable better reading of the tufts at the 10-foot radius, during the last flight a lens with a focal length of 47 millimeters was substituted in the camera in place of the original lens, the focal length of which was 24 millimeters.

The records were analyzed by plotting observations of the tuft conditions against the corresponding blade azimuth angles. The azimuth angles, ψ, at which the flow changed from unstalled to stalled and vice versa were plotted against the tip-speed ratio, μ, in figure 2. The azimuth angles at which the flow changed from stalled to reversed and vice versa are shown in figure 3. A blade section was considered stalled when the rear tuft indicated burbled flow over at least the rear 30 percent of the blade; the flow was considered reversed when the tufts pointed toward the leading edge of the blade. (See fig. 1.) The faired curves of figure 2 take into account the apparent range of uncertainty for each of the points plotted. A rough check on these curves was provided by the trailing-edge tufts but their values are omitted because of the uncertainty of their significance.

For comparison with the experimental results, theoretical stall contours for three tip-speed ratios were obtained by determining the azimuth angles at which the calculated angles of attack of various blade elements corresponded to the static stalling angle of the airfoil section. The angles of attack of a blade element at different azimuth positions were calculated by combining the calculated values of the angle of incidence, φ, of the

flow relative to the plane of the disk, with the instantaneous pitch angle, θ, of the blade element. In the determination of φ and θ, the expressions given in equations (3), (8), and (9) of reference 2 were used in conjunction with experimental values of twist and flapping coefficients.

The exact determination of the inflow factor, λ, required in the calculation of φ, is complicated by the change in blade pitch resulting from the use of upturned trailing-edge tabs on the outer part of the blades. It can be shown, however, that a substitute rotor having a uniform blade pitch of 4.5° will give identical thrust coefficients at all tip-speed ratios and, at the same time, will give values of the ratio of the torque coefficient to the thrust coefficient, C_Q/C_T, that agree reasonably well with those shown in figure 5 of reference 3 for the PCA-2 rotor when allowance is made for the greater cleanness of the YG-1B rotor. Values of λ for the substitute rotor were used in calculating φ.

The choice of 4.5° for θ is considered to be reasonably good. In order to show the effect of choosing a lower value of θ and of using the correspondingly higher value of λ and to indicate how far the change in values of θ and λ would have to be carried to produce agreement, a dotted curve representing $\theta = 3.17°$ instead of 4.5° is shown in figure 6, which will be discussed later.

The angle of attack chosen for the stall, 19.7°, measured from the zero-lift line, was based on variable-density-tunnel tests of a section obtained by fairing ordinates measured on the blades of the Kellett YG-1 autogiro. These tests showed no consistent variation of angle of stall with Reynolds Number; hence, the average value from the six tests applicable was used. The angle of attack for unstalling for many sections is lower than that for stalling, even under static conditions. The roundness of the lift-curve peaks and the absence of any abrupt drops at the peaks of the section under consideration make it unlikely that such a phenomenon would have been found had the tests covered this factor. Inasmuch as the form of the lift-curve peak might be different, even statically, under flight conditions, dotted lines are included in figures 4, 5, and 6 to show the effect of assuming a 2° "hysteresis"; that is, of assuming that stalling would occur at 19.7° and unstalling would occur at 17.7°.

RESULTS AND DISCUSSION

The results of the stalling observations are shown in figure 2, with azimuth angles for stalling or unstalling plotted against tip-speed ratio for the four values of blade radius at which the tufts were placed. Figure 7 shows the outer boundaries of the stalled areas for five tip-speed ratios, obtained by taking values from the faired curves of figure 2. The dotted portions are the ones that had to be obtained by interpolation or extrapolation. It will be noticed that the contours are roughly circular, that they cut close around the center, and that they lie almost entirely on the retreating side. The areas also consistently increase with increasing tip-speed ratio.

Outside the stalled regions, the tufts indicated the flow to be, for the most part, at least moderately smooth. Some flutter was to be expected because the tufts were nearly always yawed relative to their attachments. One peculiarity occasionally noted was the lifting of one or both tufts at 120° azimuth, that is, in the middle of the forward advancing quarter, where a real stalled region is out of the question. Although the bending or the whipping action of the blade may, for instance, cause a momentary disturbance in the flow, it seems more likely that some vagary of tuft action is appearing, for example, a fluttering when the yawing of the flow, which begins at 90° azimuth, first pries the ribbons away from the blade surface. Another peculiarity, one which is thought to be a true indication, was that the tufts at the smaller radii, especially at $x = 0.145$, showed disturbed flow practically all of the time regardless of azimuth angle or tip-speed ratio. It is also of interest that, except when indicating the section to be stalled, the pictures of the tufts showed not nearly so much foreshortening as the calculated yaw angles would indicate. The forward tufts were usually not noticeably foreshortened even when the rear tufts indicated a stall. This phenomenon checks with smoke-flow observations, which have shown yawed flow to bend more nearly parallel to the blade chord while crossing the wing surface, and supports the assumption, found to be of practical use in theoretical treatments of rotors, that the radial components of horizontal velocities can be neglected. Although both tufts occasionally appeared to relax slightly in advance of the stall, the pictures usually gave the impression that the stall spreads forward from the trailing edge.

Experimentally determined values of the azimuth angles of blade elements entering and leaving the reversed-velocity region are plotted against tip-speed ratio in figure 3. Theoretical values are included for comparison. Values taken from the faired experimental curves of figure 2 at three tip-speed ratios and the corresponding theoretical contours are shown in figure 8. In both methods of presentation, the agreement is good and, since in this instance the theory cannot be appreciably in error, the observations are evidently accurate. The entry into the reversed-velocity region was definite; the tufts had been raised by the stalled flow and streamed forward so quickly that the tuft image was blurred. Because of the reversal of flow on the blade upper surface associated with the stall, the velocity was considered not to be reversed until the forward tuft was stretched out toward the leading edge. When the section left the reversed-velocity region, however, the action was less rapid; the tufts wadded up while they were within the region and, for exact readings, it was necessary to observe the shifting of the bulk of each tuft back of its point of attachment.

The theoretically calculated boundaries of the stalled region give the same general picture as the experimental boundaries although the detailed differences are considerable. Figures 4, 5, and 6 show both theoretical and experimental results for $\mu = 0.15$, 0.25, and 0.35, respectively. The more important of the known or suspected sources for the differences between the theory and experiment follow.

First, several sources of the discrepancies are inherent in the theoretical treatment used and arise from the assumptions made in the theory. The inflow is assumed to be uniform over the rotor disk and the radial components of the horizontal velocities are neglected. The section characteristics are assumed to be unaffected by the rate of change of attack angle, which rate of change, according to the theory, reaches extremely high values near the stall boundaries. It is also assumed that an equivalent uniform pitch can be used in calculating inflow although the pitch varies somewhat with both azimuth position and radius. The neglect of radial components results in two distinct assumptions: (1) that the resulting air-speed error can be neglected; and (2) that the difference in section characteristics caused by the yaw angle actually present can be neglected. The average yaw angles, in the region between the experimental and the theoretical boundaries,

were found by calculation to be about 50° at stall and 55° at unstall. These angles are relatively unimportant at the maximum radius stalled and do not exceed 25° in any individual case.

Second, accidental errors occur in the experimental treatment; these errors chiefly increase the scatter of the plotted points. Flying directly away from the sun was difficult but, from prior experience, the resulting error was thought to be ±5° or less. In the analysis of the data, errors, apparently quite small, occurred in reading the azimuth position from the image of the sun and from the inability to compensate between these images for changes in the speed of the camera. More important, it was found difficult, if not impossible, to be entirely consistent in the interpretation of the appearance of the tufts; this lack of consistency constitutes accidental error insofar as it was caused by overexposure of the film by the sun blur caused by blade motion, and irregular attachment of the tufts. None of these accidental errors apparently had any truly primary importance because the average deviation of the individual points from the faired curves of figure 2 is ±6°. This deviation includes the scatter that variations in the air flow, or perhaps in the tuft response, apparently produced if judged from comparison of repeat runs.

Third, systematic errors are present in the experiment. Lag in the response of the tufts to the air flow was expected to be the most important of these systematic errors. It was thought that, under the varying conditions present and particularly the varying relative velocities, the lag might identify itself by producing absurdities, but it did not. Such lag would not only shift the stall and the unstall indications to larger azimuth angles and by unequal amounts but also decrease the maximum radius shown to be stalled through failure of the tufts to respond at all if the time of the stall were too brief. This decrease in the maximum radius is minimized somewhat by the fact that the extreme outer ends of the contours represent extrapolation, for the most part, of stalled values and is further minimized by the existence of brief, weak stall indications at several tip-speed ratios below the closures of the curves of figure 2, which is in a sense equivalent to stall indications at a greater radius at a given tip-speed ratio. The supposed importance of tuft lag was considerably minimized by the results of the reversed-velocity comparison. (See figs. 3 and 8.)

The presence of the tuft and its attachment must also necessarily change the flow to some degree. A study of the literature on the effect of protuberances together with a consideration of the rapidity and the general nature of the spread of the stall on the blades suggests, but by no means proves, that this factor is negligible. Another source of error is the difficulty of correctly interpreting the appearance of the tufts. It was found necessary to interpret their entering and leaving the region of stall on different bases. When the blade element entered the stalled region, it was assumed to be stalled when the tuft disturbance, which was evident first at the trailing edge, had spread forward to a point 70 percent back of the leading edge. This tuft condition was assumed to coincide with separation of the air flow from the blade surface over the rear 30 percent of the section. When the blade element leaves the stalled region, theory predicts that the angles of attack will drop abruptly to extremely low values. The blade elements were therefore regarded as stalled until the tufts indicated an air flow corresponding to low angles of attack. The choice of a 30-percent advance of the separation point as a definition of entry into the stalled region was arbitrarily made for the reason that present knowledge permits no accurate correlation of separation point and lift-coefficient values under the conditions of operation of the rotor. Fortunately, the entry values are not critically affected by the point chosen.

The primary difference found between experiment and theory in regard to the stalled region is simply that experiment indicates this region to be larger and more important than is suspected from theory. It is convenient to break the difference up into three phases: (1) stalling, (2) unstalling, and (3) maximum radius stalled.

The discrepancy between theory and experiment during the stalling phase was markedly the smallest on the basis of azimuth angles or of areas; in fact, a rough agreement may be considered to exist. If the discrepancy is judged on another basis, namely, the departure of the theoretical value of the angle of attack of the stalling element from the static value, 19.7°, the agreement still is much better than for the unstalling phase but approaches the degree of discrepancy present in the maximum-radius region. These average angle-of-attack deviations were 3.8°, 4.2°, and -1.5° for $\mu = 0.15$, $\mu = 0.25$, and $\mu = 0.35$, respectively, the minus sign indicating an angle of attack less

than 19.7°. It is unknown, of course, to what extent the deviations are due to erroneous theoretical angle-of-attack values or to what extent they are due to variation of the section characteristics from the static values used; however, both sources are certainly present. An appreciable portion of the deviations also undoubtedly results from experimental error but, in this phase, the experiment is thought to be fairly trustworthy and at least to be more reliable than the theory. The discrepancy may also be expressed in blade chord lengths traveled relative to the air; on this basis, average values of 1.0, 0.5, and -0.4 blade chords, respectively, are obtained for the three tip-speed ratios being considered. Corresponding average air speeds for the zones in which the discrepancy exists are 70, 110, and 170 feet per second; these are the resultant velocities and not the components perpendicular to the blade spar. They were obtained by averaging values calculated at several points along the theoretical and the experimental boundaries in the stalling phase.

The discrepancy in the unstalling phase is far larger than that in the stalling phase on the basis of azimuth angle, area, or blade chord lengths. It approximately equals the discrepancy in the maximum-radius-stalled phase with regard to the area. This difference may, however, represent the smallest amount of energy loss because the angles of attack are apparently quite low and the force coefficients may therefore be suspected of being fairly low also, even if the flow is in a disturbed condition. Average deviations in azimuth angle are 68°, 58°, and 51°, respectively, for the three values of μ; average deviations in blade chord length are 2.9, 3.2, and 3.1; and average velocities are 70, 100, and 160 feet per second. Angle-of-attack differences lose their significance in this zone because the smaller radii at the higher tip-speed ratios unstalled from a negative angle of attack acquired while they were within the reversed-velocity region. The average angle-of-attack values corresponding to unstalling were 10°, 6°, and 4° for the three tip-speed ratios, respectively.

The differences in the maximum radius stalled are almost unquestionably of most importance with regard to energy loss and also appear to be the easiest to correct. They are, further, the most reliable indication of errors in the theoretically determined boundaries; the source of error that causes most concern in the other phases cannot account for this difference because lag in tuft response

would reduce rather than increase the maximum radius stalled. Expressed as fractions of blade radius, the excesses indicated by experiment were 0.05, 0.125, and 0.15 in order of increasing tip-speed ratio. Corresponding average velocities at the outer ends of the boundaries were 80, 95, and 115 feet per second; average velocities for the areas represented would be roughly one third larger. Angle-of-attack differences are -7.2°, -5.7°, and -3.7° when determined as previously described. It is of interest to note that the section at the tip of the experimental boundary has passed the azimuth value at which theory shows it to have the highest attack angle. These highest values of attack angle are still below 19.7°; the differences are -3.7°, -4.7°, and -3°. The important items about the maximum-radius-stalled zones are: (1) a large amount of energy is represented because of the extremely high drag coefficients that apply beyond the stall, the large average velocities, and the large areas represented; and (2) approximately 5° increase in the angle of attack for the stall of the sections affected should serve to wipe out the waste represented. These statements are especially applicable to the higher tip-speed ratios. The 5° increase would need to apply over only a part of the blade, roughly from 0.3 to 0.6 of the radius, which suggests the desirability of special treatment of this section without adversely affecting the low-drag characteristics of the outer portions of the blades.

Attempts to correlate the differences between theory and experiment with the air velocity, the yaw angle, or the rate of change of the angle of attack proved futile. Agreement was also impossible to obtain by a fixed change in angle of attack assumed for the stall, by a fixed change in the inflow coefficient used, or by assuming hysteresis in conjunction with either. The difference in unstalling was roughly constant when expressed in blade chord lengths. If this factor is assumed to be fixed and correct, then, by means of a moderate decrease in angle of attack for the stall together with a moderate increase in inflow coefficient (that is, a value between the two used), agreement can be obtained for $\mu = 0.35$. There is no justification in the theory, however, for increasing the inflow beyond the lower of the two values used nor would the treatment function for the lower tip-speed ratios. The inflow is not actually uniform over the disk; this nonuniformity might account for at least a part of the observed discrepancies except those in the unstalling phase, where it could scarcely be of sufficient magnitude to have an effect and

is thought to act in the wrong direction. In brief, the discrepancies in stalling and maximum-radius-stalled values must be ascribed to a mixture of factors of unknown relative importance; whereas, those in unstalling values must be chiefly laid to aerodynamic lag of flow pattern. The known weaknesses of the theory, together with the favorable check of the experimental method given by the reversed-velocity study, lead to the conclusion that the experimental contours are more trustworthy than the theoretical ones, in spite of the unknown interference effects caused by tufts.

The tuft method of obtaining stall contours appears to work well enough to justify further use, particularly as a means of checking attempted reductions of stalled regions. A number of improvements in the method should be possible. Further experiment should reveal some combination of tuft size, form, method of attachment, and location appreciably superior to this preliminary arrangement, especially with regard to the certainty of indication by the tufts. Before further observations are undertaken, such devices as pivot attachments, attachment on posts, use of lighter or fluffier tuft material, and use of more tufts should be investigated. The camera set-up could also be improved to produce clearer pictures; a faster shutter speed, a longer focal length of lens, and the determination of azimuth by the use of some means other than the sun would reduce blurring and overexposure.

CONCLUSIONS

1. Experiment and theory agree with regard to the shape and the general location of the stalled area on the Kellett YG-1B autogiro rotor.

2. The stalled regions on the YG-1B autogiro rotor are larger than simple theory indicates.

3. At the higher tip-speed ratios, the stalled region is large enough to be a possible factor in both the rotor lift-drag ratio and the blade flapping motion.

4. The tuft method of observation is effective enough to be helpful in studies of the stalled region.

Langley Memorial Aeronautical Laboratory,
National Advisory Committee for Aeronautics,
Langley Field, Va., November 30, 1939.

REFERENCES

1. Wheatley, John B.: An Analysis of the Factors that Determine the Periodic Twist of an Autogiro Rotor Blade, with a Comparison of Predicted and Measured Results. T.R. No. 600, N.A.C.A., 1937.

2. Wheatley, John B.: An Analytical and Experimental Study of the Effect of Periodic Blade Twist on the Thrust, Torque, and Flapping Motion of an Autogiro Rotor. T.R. No. 591, N.A.C.A., 1937.

3. Bailey, F. J., Jr.: A Study of the Torque Equilibrium of an Autogiro Rotor. T.R. No. 623, N.A.C.A., 1938.

(a) Blade at 45° azimuth; $\mu = 0.319$; flow undisturbed.

(b) Blade at 215° azimuth; $\mu = 0.319$; flow reversed at 3-foot radius; stalled at 5-foot radius, and approaching stall at 10-foot radius.

Figure 1.- Typical tuft-photographs over blades of the YG-1B autogiro rotor.

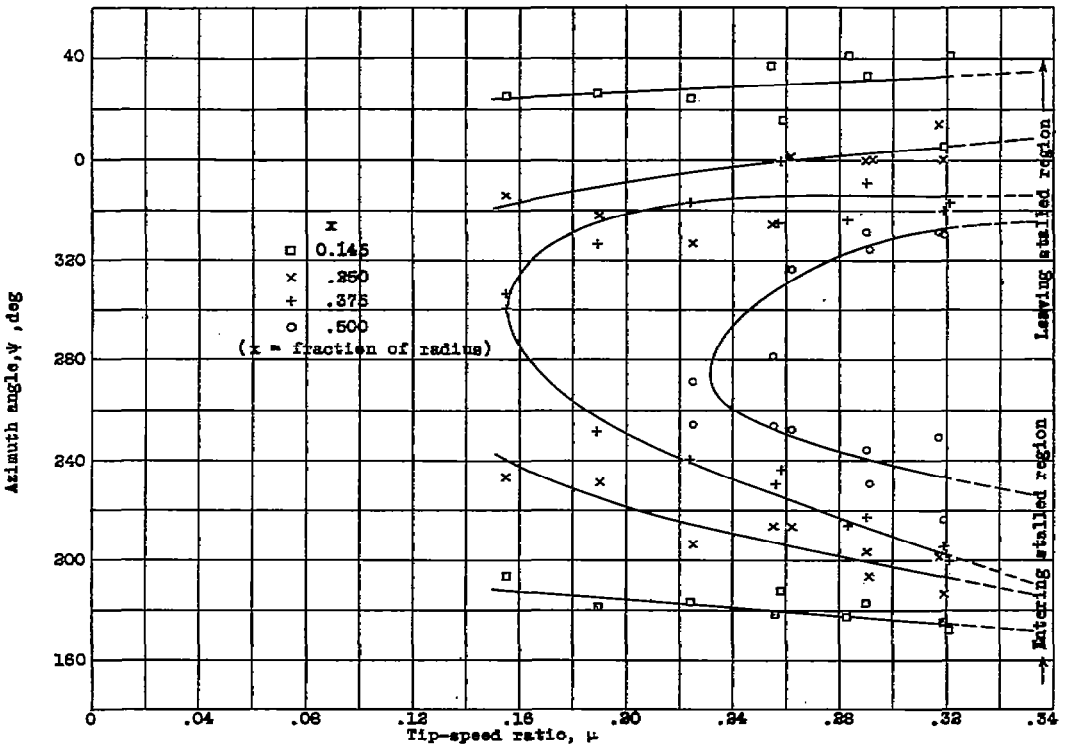

Figure 2.- Experimental values of the azimuth angles at which the blade element enters and leaves the region of stalled flow. The YG-1B autogiro rotor.

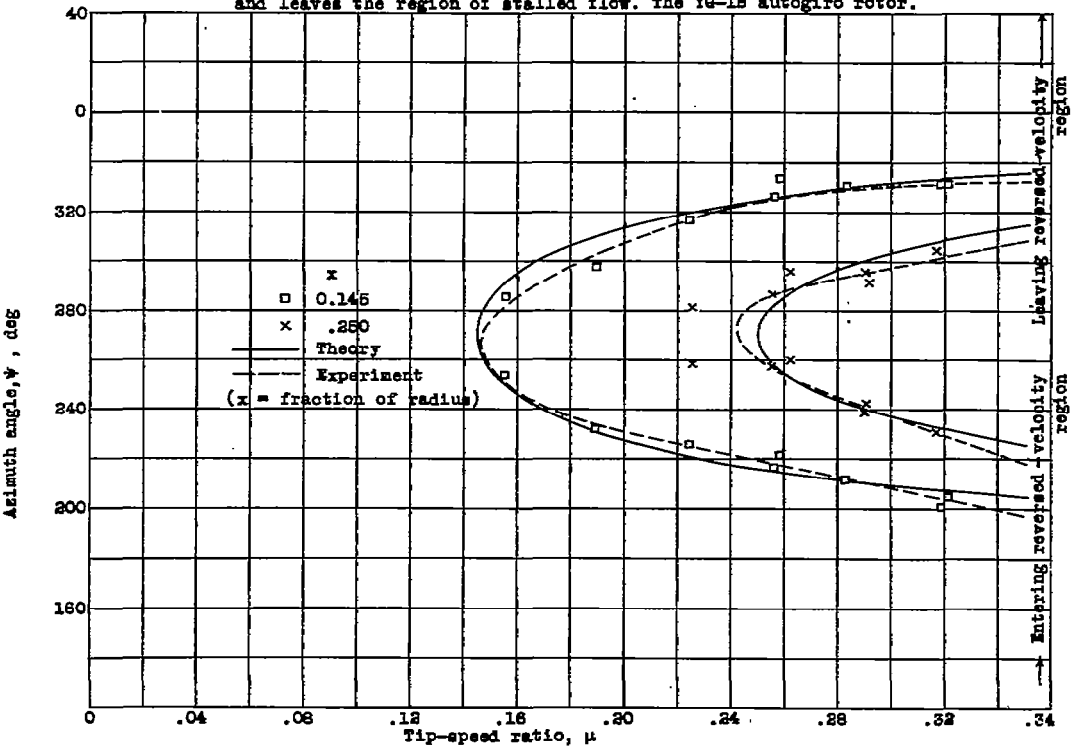

Figure 3.- Experimental values of the azimuth angles at which the blade element enters and leaves the reversed-velocity region. The YG-1B autogiro rotor.

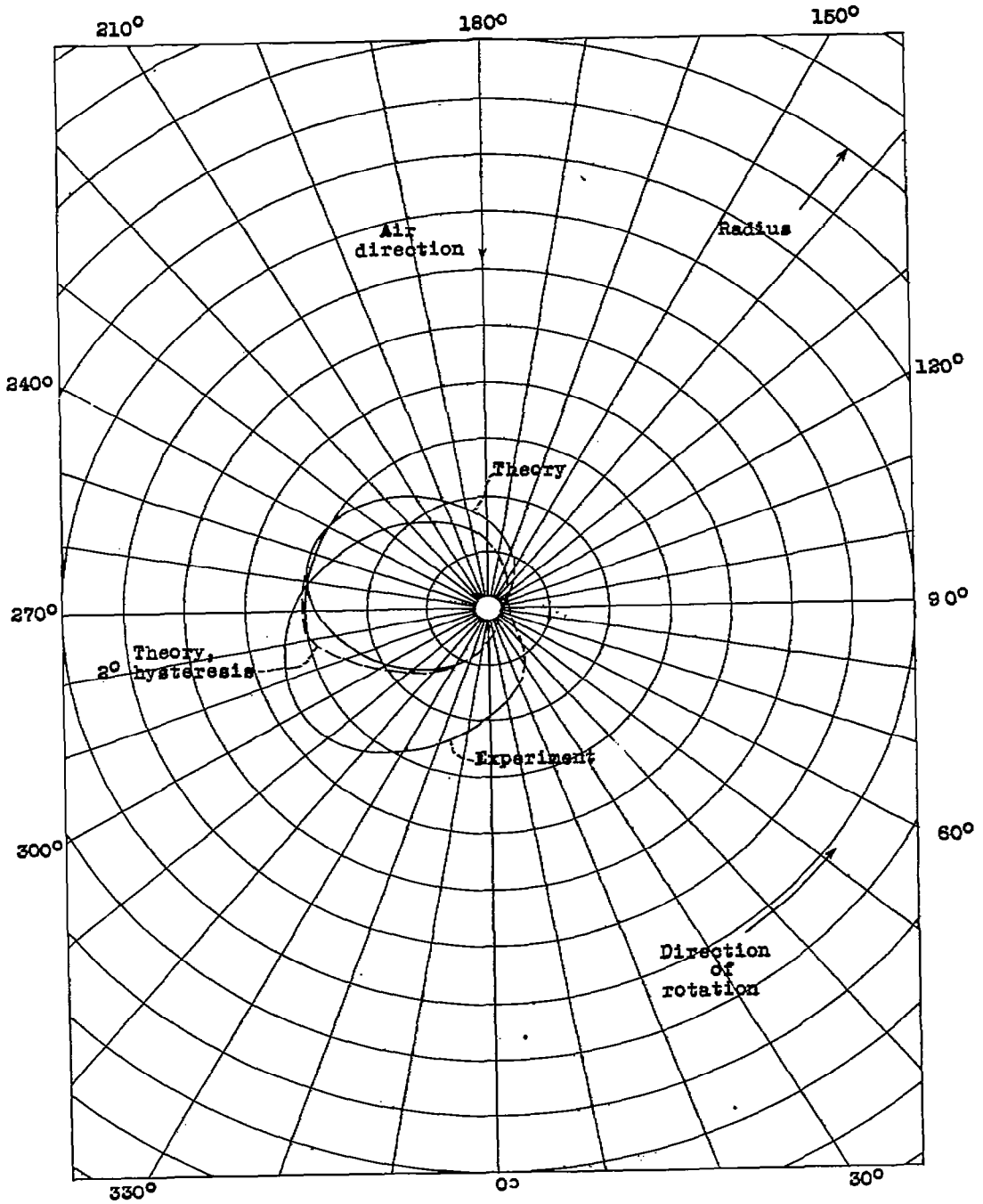

Figure 4.- Experimental and theoretical outer boundaries of the region of stalled flow for $\mu = 0.15$. The YG-1B autogiro rotor.

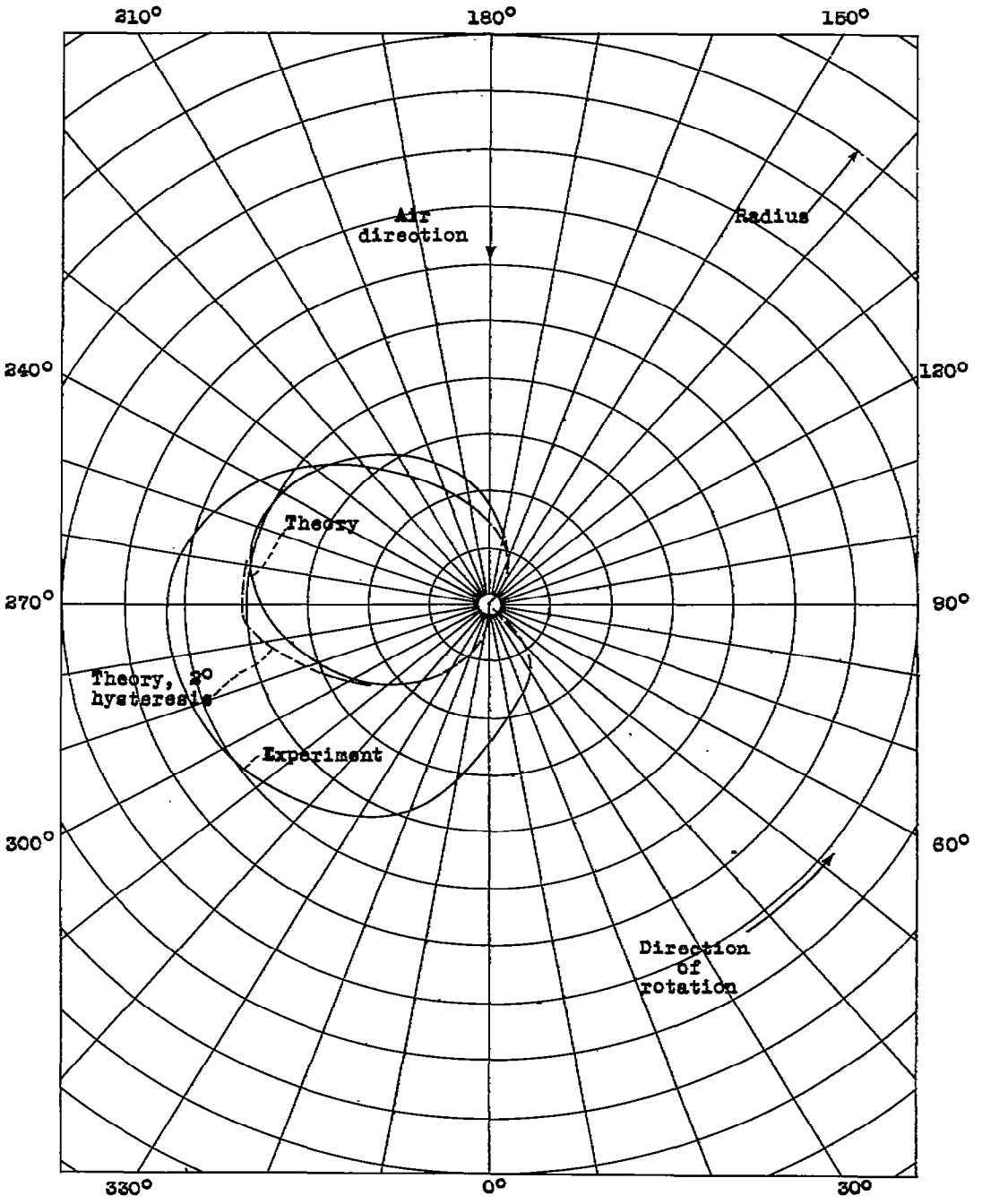

Figure 5.- Experimental and theoretical outer boundaries of the region of stalled flow for $\mu = 0.25$. The YG-1B autogiro rotor.

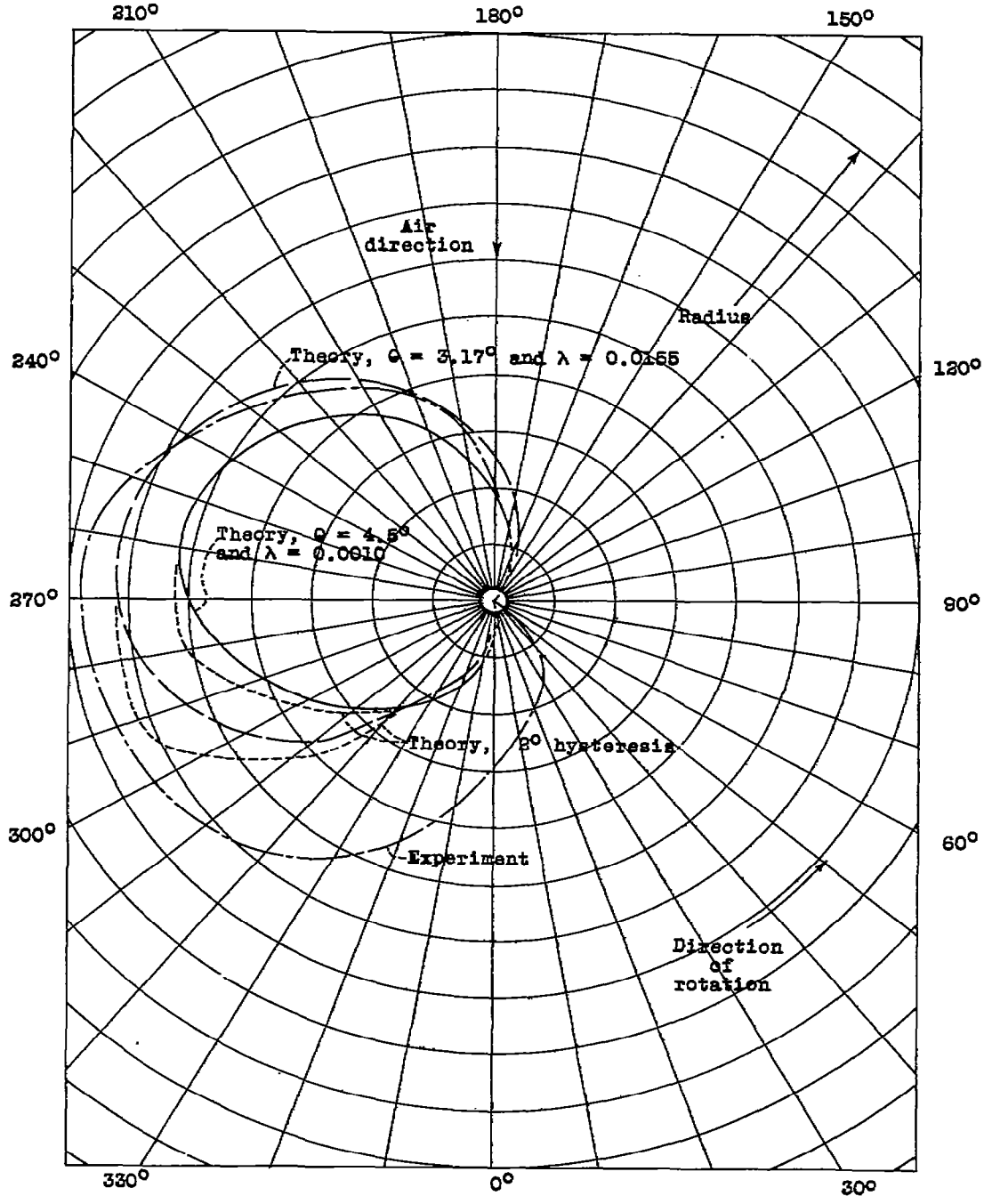

Figure 6.- Experimental and theoretical outer boundaries of the region of stalled flow for $\mu = 0.35$. The YG-1B autogiro rotor.

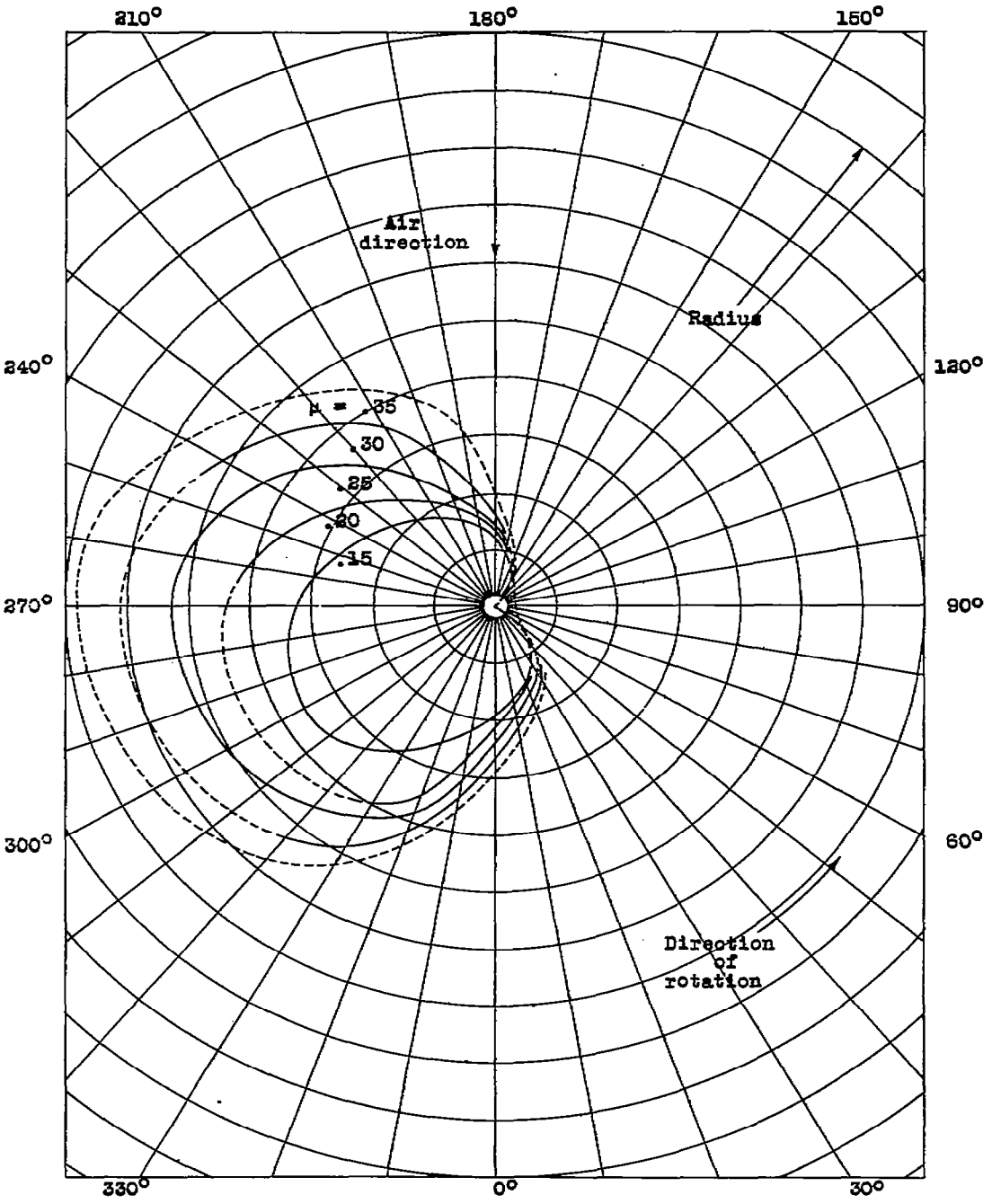

Figure 7.- Experimental outer boundaries of the region of stalled flow as obtained from the tuft observations. The YG-1B autogiro rotor.

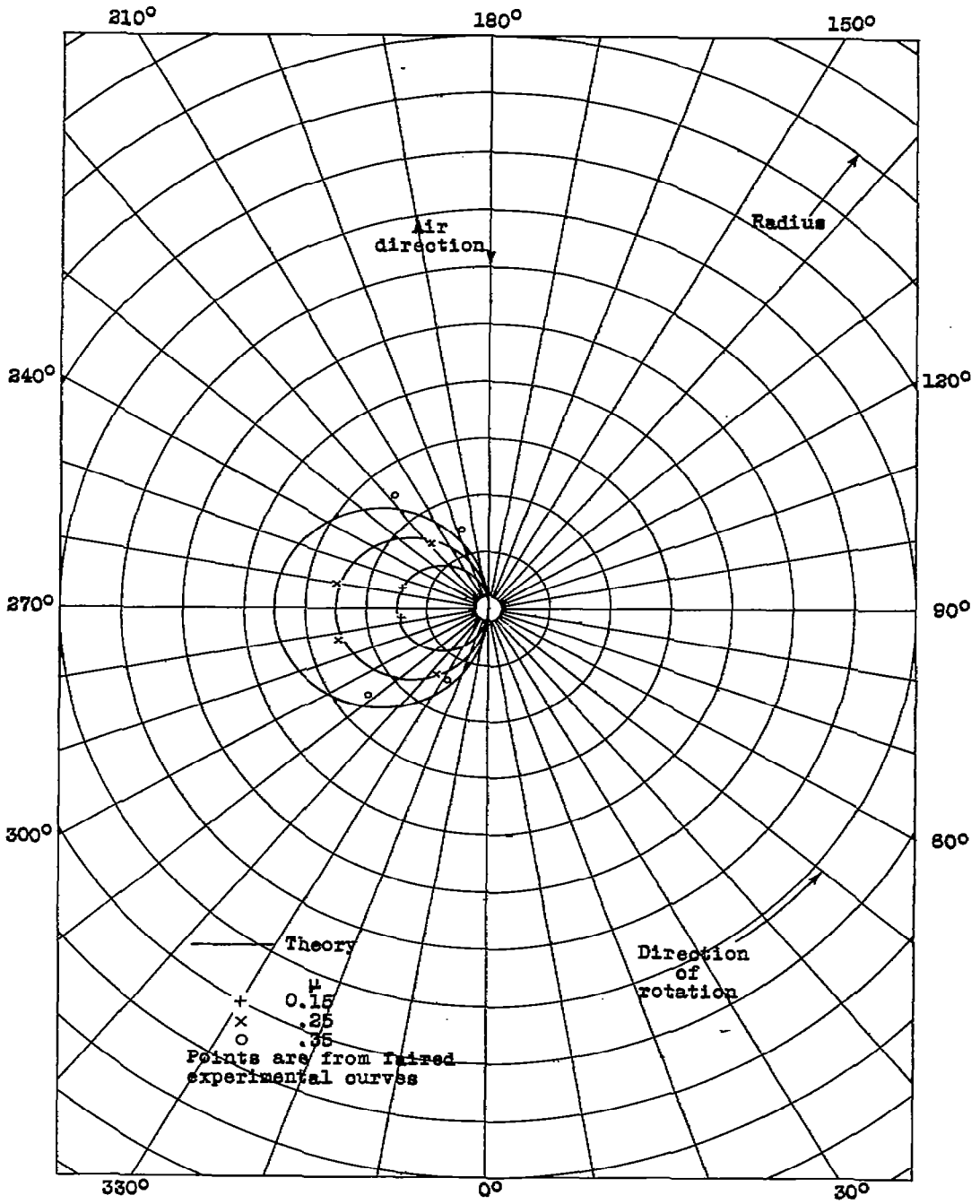

Figure 8.- Comparison of experimental velocity-reversal values with theoretical boundaries of the reversed-velocity region for three tip-speed ratios. The YG-1B autogiro rotor.